
This copy is for your personal, non-commercial use only.

If you wish to distribute this article to others, you can order high-quality copies for your colleagues, clients, or customers by [clicking here](#).

Permission to republish or repurpose articles or portions of articles can be obtained by following the guidelines [here](#).

The following resources related to this article are available online at www.sciencemag.org (this information is current as of October 3, 2014):

Updated information and services, including high-resolution figures, can be found in the online version of this article at:

<http://www.sciencemag.org/content/346/6205/81.full.html>

Supporting Online Material can be found at:

<http://www.sciencemag.org/content/suppl/2014/10/01/346.6205.81.DC1.html>

A list of selected additional articles on the Science Web sites **related to this article** can be found at:

<http://www.sciencemag.org/content/346/6205/81.full.html#related>

This article **cites 33 articles**, 7 of which can be accessed free:

<http://www.sciencemag.org/content/346/6205/81.full.html#ref-list-1>

This article has been **cited by** 1 articles hosted by HighWire Press; see:

<http://www.sciencemag.org/content/346/6205/81.full.html#related-urls>

This article appears in the following **subject collections**:

Physiology

<http://www.sciencemag.org/cgi/collection/physiology>

the time required to hunt (Fig. 2), our model suggests that, unlike wild dogs, cheetahs are able to cope with kleptoparasitism rates of 25%, because this would only require an additional 1.1 hour per day (a 38% increase) in time spent mobile and increase DEE to 10.0 MJ per day (a 12% increase). Wild dogs may be exceptional in this regard because the high power costs ($25 \times$ RMR, 35 W/kg) and long durations of prey pursuits (3.5 hours per day) make their hunting strategy extremely costly. This contrasts with the hunting strategy of cheetahs; even though power use during pursuit may reach 120 W/kg (19), prey pursuit takes only a few seconds and constitutes a small component of the daily energy budget (undetected here using doubly labeled water).

Recorded rates of kleptoparasitism in cheetahs are lower than the untenable threshold of over 50% (Fig. 2): 14% in Kruger National Park (24), 11% in the Serengeti (25), and 9.3% in the Kgalagadi Transfrontier Park (current study). Relatively low kleptoparasitism rates in cheetahs that do not change greatly between ecosystems may be due to effective competitor avoidance strategies (9) and a diurnal hunting strategy (26). The comparatively low cost of food acquisition and flexible energy budget of cheetahs compared with that of wild dogs (6) are likely to provide a buffer against varying ecological conditions.

This study lends support to suggestions that interspecific competition does not necessarily suppress cheetah populations (27–30). Instead, it shows that cheetahs are well adapted to the presence of competitors and that costs incurred by traveling drive their energy budgets, rather than those encountered securing prey. Human activities that force cheetahs to travel large distances to avoid disturbance and persecution may push DEE to the limit and consequently compromise their population viability.

REFERENCES AND NOTES

- M. M. Humphries, K. S. McCann, *J. Anim. Ecol.* **83**, 7–19 (2014).
- C. Carbone, A. Teacher, J. M. Rowcliffe, *PLoS Biol.* **5**, e22 (2007).
- S. Tomlinson *et al.*, *Trends Ecol. Evol.* **29**, 280–290 (2014).
- C. Carbone *et al.*, *Biol. Lett.* **7**, 312–315 (2011).
- W. J. Ripple *et al.*, *Science* **343**, 1241484 (2014).
- M. L. Gorman, M. G. L. Mills, J. P. Raath, J. R. Speakman, *Nature* **391**, 479–481 (1998).
- T. M. Caro, *Cheetahs of the Serengeti Plains* (Univ. of Chicago Press, Chicago, 1994).
- S. M. Durant, *J. Anim. Ecol.* **67**, 370–386 (1998).
- S. M. Durant, *Behav. Ecol.* **11**, 624–632 (2000).
- M. G. L. Mills, M. L. Gorman, *Conserv. Biol.* **11**, 1397–1406 (1997).
- S. R. Creel, N. M. Creel, *Conserv. Biol.* **10**, 526–538 (1996).
- G. B. Schaller, *The Serengeti Lion. A Study of Predator-Prey Relations* (Univ. of Chicago Press, Chicago, 1972).
- M. G. L. Mills, *Kalahari Hyenas: Comparative Behavioral Ecology of Two Species* (Springer, Dordrecht, 1990).
- S. Creel, N. M. Creel, *The African Wild Dog: Behaviour, Ecology and Conservation* (Princeton Univ. Press, Princeton, 2002).
- A. Hilborn, N. Pettorelli, C. D. L. Orme, S. M. Durant, *Anim. Behav.* **84**, 701–706 (2012).
- J. W. Wilson *et al.*, *Biol. Lett.* **9**, 20130620 (2013).
- C. Carbone, G. M. Mace, S. C. Roberts, D. W. Macdonald, *Nature* **402**, 286–288 (1999).
- M. W. Hayward, M. Hofmeyr, J. O'Brien, G. I. H. Kerley, *J. Zool.* **270**, 615–627 (2006).
- A. M. Wilson *et al.*, *Nature* **498**, 185–189 (2013).
- J. R. Speakman, *Doubly-Labelled Water* (Chapman & Hall, London, 1997).
- C. C. Peterson, K. A. Nagy, J. Diamond, *Proc. Natl. Acad. Sci. U.S.A.* **87**, 2324–2328 (1990).
- J. S. Brown, B. P. Kotler, *Ecol. Lett.* **7**, 999–1014 (2004).

- J. du P. Bothma, E. A. N. le Riche, *J. Arid Environ.* **18**, 79–84 (1990).
- M. G. L. Mills, H. C. Biggs, *Symp. Zool. Soc. London* **65**, 253–268 (1993).
- J. S. Hunter *et al.*, *Behav. Ecol. Sociobiol.* **61**, 1033–1042 (2007).
- T. M. Caro, in *Mammals of Africa Volume V*, J. Kingdon, M. Hoffmann, Eds. (Bloomsbury, London, 2013), pp. 186–196.
- F. Broekhuis, G. Cozzi, M. Valeix, J. W. McNutt, D. W. Macdonald, *J. Anim. Ecol.* **82**, 1098–1105 (2013).
- M. G. L. Mills, M. E. J. Mills, *J. Zool.* **292**, 136–141 (2014).
- G. Cozzi *et al.*, *Ecol.* **93**, 2590–2599 (2012).
- A. Swanson *et al.*, *J. Anim. Ecol.* **10.1111/1365-2656.12231** (2014).
- J. R. Speakman, E. Kröl, *J. Anim. Ecol.* **79**, 726–746 (2010).
- I. Capellini *et al.*, *Ecology* **91**, 2783–2793 (2010).
- L. N. Hudson *et al.*, *J. Anim. Ecol.* **82**, 1009–1020 (2013).
- A. A. Degen, M. Kam, *Ecoscience* **2**, 48–54 (1995).

ACKNOWLEDGMENTS

The data reported in this paper are presented in the supplementary materials (table S1). This study was supported by the Royal Society (2009/R3 JP090604) and Natural Environment Research Council (NE/I002030/1) to D.M.S. J.R.S. was supported by the Strategic Priority Research Program of the Chinese Academy of Sciences (XDB13030000) and a 1000 Talents professorship. We thank SANParks and the Department of Wildlife and National Parks, Botswana, for allowing our research in the Kgalagadi Transfrontier Park (Permit Number 2006-05-01 to M.G.L.M.) and

the Lewis Foundation, South Africa; The Howard G. Buffet Foundation; National Geographic; Kanabo Conservation Link; Comanis Foundation; Panthera; and the Kruger Park Marathon Club for financial support to M.G.L.M. J.W.W. was funded by NASA grants NNX11AP61G and NNX11AL49H. We thank the management and land owners of Karongwe Game Reserve, as well as the directors of Karongwe Game Association, for supporting this research on their land. We are also grateful to the many Global Vision International field staff and volunteers who conducted the Karongwe fieldwork. We thank I. Capellini for providing additional information on DEE allometry and C. Hambly and P. Thomson for technical assistance with the isotope analysis. Author contributions: D.M.S., M.G.L.M., J.W.W., M.E.J.M., P.B., and N.J.M. collected data; J.R.S. analyzed isotopes; D.M.S., M.G.L.M., R.P.W., and J.W.W. analyzed data; and D.M.S., M.G.L.M., R.P.W., J.W.W., M.E.J.M., S.M.D., N.C.B., P.B., N.J.M., and J.R.S. wrote the manuscript.

SUPPLEMENTARY MATERIALS

www.sciencemag.org/content/346/6205/79/suppl/DC1
Materials and Methods
Figs. S1 and S2
Table S1
References (35–53)

23 May 2014; accepted 11 August 2014
10.1126/science.1256424

MAMMALIAN ENERGETICS

Instantaneous energetics of puma kills reveal advantage of felid sneak attacks

Terrie M. Williams,^{1*} Lisa Wolfe,² Tracy Davis,² Traci Kendall,¹ Beau Richter,¹ Yiwei Wang,³ Caleb Bryce,¹ Gabriel Hugh Elkaim,⁴ Christopher C. Wilmers³

Pumas (*Puma concolor*) live in diverse, often rugged, complex habitats. The energy they expend for hunting must account for this complexity but is difficult to measure for this and other large, cryptic carnivores. We developed and deployed a physiological SMART (species movement, acceleration, and radio tracking) collar that used accelerometry to continuously monitor energetics, movements, and behavior of free-ranging pumas. This felid species displayed marked individuality in predatory activities, ranging from low-cost sit-and-wait behaviors to constant movements with energetic costs averaging 2.3 times those predicted for running mammals. Pumas reduce these costs by remaining cryptic and precisely matching maximum pouncing force (overall dynamic body acceleration = 5.3 to 16.1g) to prey size. Such instantaneous energetics help to explain why most felids stalk and pounce, and their analysis represents a powerful approach for accurately forecasting resource demands required for survival by large, mobile predators.

A central tenet of foraging theory is that animals manage energetic costs and benefits when feeding (1). Yet measuring these costs for large, highly active predators that hunt, chase, and kill mobile prey has been exceedingly difficult, resulting in a poor understanding of how physiological capacities and environmental factors affect foraging success (2).

This is especially apparent for species within the family *Felidae*. Among terrestrial carnivores, felids show a large range in body size, prey preferences, and predatory movements, each of which are linked to the landscape in which they live (3–6). The lankiest cat, the African cheetah (*Acinonyx jubatus*), engages in astonishing high-speed pursuits in open habitats to outmaneuver and overtake smaller, swift prey (7, 8). In contrast, heavy-bodied species including African lions [*Panthera leo* (9)], leopards (*Panthera pardus*), tigers (*Panthera tigris*), and pumas residing in forested or grassland habitats tend to stalk, ambush, and pounce to overpower prey up to several times their size (6).

Of the 36 extant wild felid species, the majority are considered cryptic ambush hunters

¹Department of Ecology and Evolutionary Biology, University of California, Santa Cruz, CA 95060, USA. ²Wildlife Health Program, Colorado Parks and Wildlife, 4330 West Laporte Avenue, Fort Collins, CO 80521, USA. ³Center for Integrated Spatial Research, Department of Environmental Studies, University of California, Santa Cruz, CA 95064, USA.

⁴Autonomous Systems Lab, Department of Computer Engineering, University of California, Santa Cruz, CA 95064, USA.

*Corresponding author. E-mail: williams@biology.ucsc.edu

(5, 6), which would suggest an energetic advantage for this predatory tactic (1). However, because of the covert nature of these activities, it is difficult to observe felid ambush behaviors or measure energetic efficiency. By necessity, field energetic studies of most terrestrial carnivores have relied on broad approaches, including doubly labeled water methods and field metabolic rate (FMR) modeling that integrate energetics across days or seasons [e.g., (10–12)].

Here, we monitored behavior-specific energetics of a large cryptic felid, the puma, to evaluate the cost of discrete physiological states involved with ambush hunting. Using a laboratory-to-field approach, we developed and calibrated a new SMART (species movement, acceleration, and radio tracking) wildlife collar on captive, adult pumas ($n = 3$), with subsequent deployment on wild pumas ($n = 4$ pumas with SMART collars, 1 puma with GPS only; tables S1 and S2). We created a library of behavior-specific collar acceleration signatures by filming instrumented, trained pumas as they traversed a 20-m level course at different speeds, performed routine activities (resting, eating, grooming, etc.), and ran on a motorized treadmill (13). Accelerometer signatures were then correlated to energetic costs by simultaneously measuring oxygen consumption (\dot{V}_{O_2}), kinematics [stride frequency, stride length (14)], and overall dynamic body acceleration [ODBA (2, 15)] of the pumas during steady-state resting and treadmill running. Cost of transport (COT, the energy expended per meter) and cost of acceleration (COA, the energy ex-

pended per g) were calculated by dividing \dot{V}_{O_2} by speed and ODBA, respectively.

In the field, we captured and instrumented wild pumas ($n = 2$ females, 2 males) with the calibrated SMART collar. An additional female instrumented with a GPS collar allowed for a detailed analysis of hunting movements and longer deployment due to the conservation of collar batteries. All pumas were then released into a 1700-km² study area within the Santa Cruz Mountains of California. The collar integrated a three-axis accelerometer and magnetometer that continuously monitored activity level and body position at 64 Hz, with a GPS/VHF unit with remote download capabilities that sampled every 4 hours to provide movement and kill locations (13). Potential kill sites were initially identified by the clustering of GPS positions indicating a feeding event, using a custom program integrated in ArcGIS (v.10; ESRI, 2010). Carcass visitation based on the GPS data allowed positive prey identification (13, 29). The timing of the GPS cluster was then correlated to time-synched accelerometer signals and behavioral signatures that indicated a pouncing event. Together, the suite of data from the collar allowed us to map both physiological and behavioral responses of wild pumas onto the physical landscape in which they hunted.

Our results indicate that the biomechanics and energetics of running by pumas are typical of most quadrupedal mammals including other adult felids (16). Both stride frequency and stride length of pumas increased linearly with running speed (Fig. 1A). Pumas also switched among

walking, trotting, and running gaits at transition speeds predicted for their body mass (17). Routine preferred speed on the outdoor course and treadmill was 1.1 m s⁻¹; maximum speed (4.9 m s⁻¹) was only one-fifth of that measured for cheetahs chasing prey (7, 8).

The oxygen consumption (ml O₂ kg⁻¹ min⁻¹) of pumas increased linearly with running speed (m s⁻¹; Fig. 1B) according to

$$\dot{V}_{O_2} = 8.15 + 10.99(\text{speed})$$

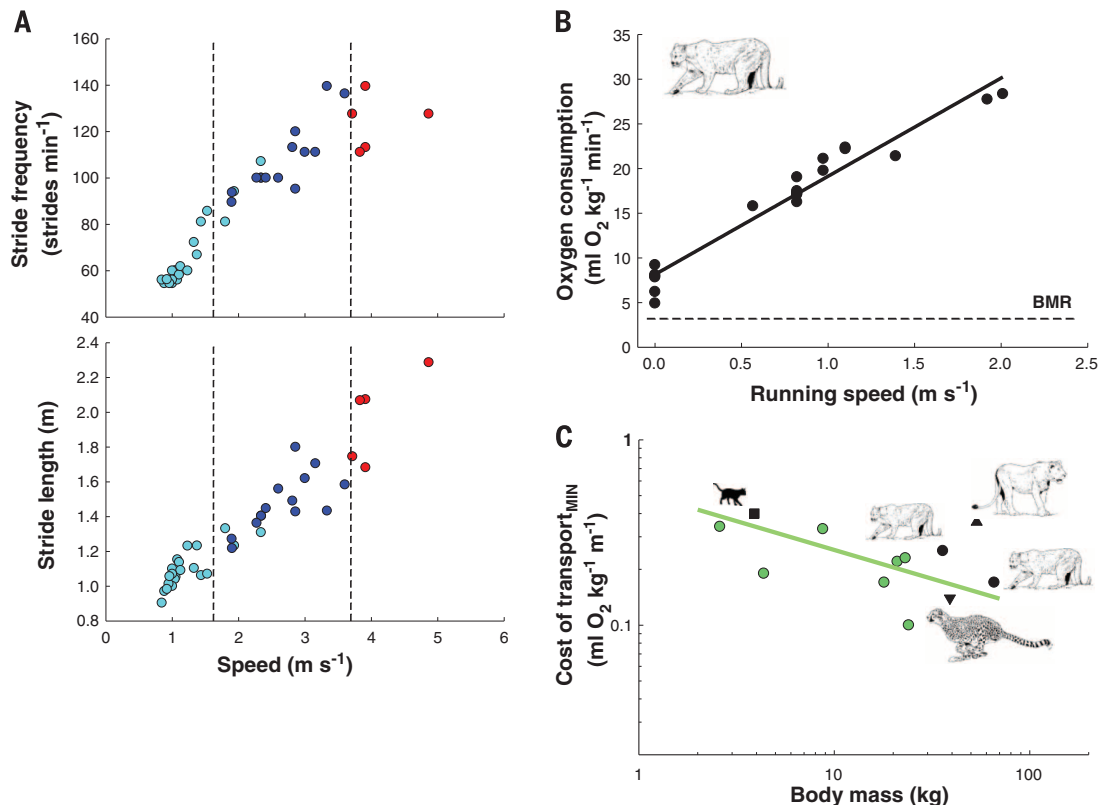
$$(r^2 = 0.95, n = 20, P < 0.0001) \quad (1)$$

Minimum cost of transport (COT_{MIN}) was 0.17 ml O₂ kg⁻¹ m⁻¹ (3.42 J kg⁻¹ m⁻¹), as predicted for canids and other felids on the basis of body mass (Fig. 1C) (16). This includes large and small felids that stalk, pounce, and perform high-speed chases. Immature African lions, however, are outliers with a COT_{MIN} that is 2.4 times that predicted for running mammals (18) and 2.1 times the value for pumas. If adults follow the trend for immature lions, then comparatively high locomotory costs of African lions may help to explain the tendency of this species to rely on cooperative hunting, which is unique among felids (6).

Continuous monitoring of acceleration in wild pumas wearing SMART collars allowed us to determine how these costs vary with hunting across time and space for individuals. Figure 2A shows a typical GPS track on the day of a kill for a 42-kg female puma hunting black-tailed deer (*Odocoileus hemionus*). The cat moved downhill through a residential area, stalked and killed

Fig. 1. Stride mechanics and energetic costs of running pumas.

(A) Stride frequency and stride length in relation to outdoor speed ($n = 3$ pumas). Points represent individual walk (cyan), trot (blue), or run (red) trials. Dashed lines show predicted gait transition speeds (17). **(B)** Oxygen consumption in relation to speed for pumas on a treadmill. Points represent individual steady-state measurements. The least-squares regression (solid line, Eq. 1) is compared to basal metabolic rate [BMR, dashed line; (25)]. **(C)** Minimum cost of transport (COT) for canids [green circles (16)], pumas [black circles, present study and (30)], and other felids [domestic cat, black square; African lion, upward triangle; African cheetah, downward triangle (16)]. The green line is the allometric regression for COT_{MIN} of quadrupeds (16).



a deer, and stayed within 200 m of the carcass until moving into the mountains the next day. What is not apparent in such GPS tracks is the considerable variation in behaviors and energy expended by a puma when pursuing different-sized prey. Here the continuous, high-resolution time-stamped accelerometer traces from the SMART collar provide remarkable insight. First, unique accelerometer signatures within the traces reveal individual behaviors that can be localized via GPS on the terrain where they occur (Fig. 2A). Second, raw triaxial acceleration traces (Fig. 2A, bottom) can be collapsed into overall dynamic body acceleration (ODBA) values and then transformed into activity-specific metabolic costs in terms of $\dot{V}O_2$ ($\text{ml O}_2 \text{ kg}^{-1} \text{ min}^{-1}$) using the regression

$$\dot{V}O_2 = 3.52 + 58.42(\text{ODBA})$$

$$(r^2 = 0.97, n = 9, P < 0.0001) \quad (2)$$

from the instrumented pumas walking on a treadmill (Fig. 2B) (13).

Equation 2 allows the acceleration signatures of wild pumas to be assigned to the energetic cost associated with each behavior. As reported for smaller animals and humans (15, 19), pumas

show a significant, linear correlation between oxygen consumption and ODBA. Like COT (16), COA declines asymptotically with ODBA (Fig. 2B, inset), showing a decline in the variation of acceleration costs as activity level increases (i.e., <10% change in COA with ODBA from 0.5 to 3.0 g). The lowest COA ($\sim 58 \text{ ml O}_2 \text{ kg}^{-1} \text{ min}^{-1}/\text{g}$ ODBA) occurs at the highest ODBA and is equivalent to the slope of the relationship in Eq. 2. Together, these relationships enable energetic costs to be ascribed to a wide variety of aerobic activities as long as ODBA accurately reflects the puma's movements (2, 15, 19).

Using these methods, we assigned energetic costs for pumas during three characteristic periods: (i) pre-kill activity (locating prey), (ii) pounce and kill, and (iii) post-kill prey handling and eating. These periods constitute a characteristic 2-hour interval we term the "hunt" (Fig. 2 and Fig. 3). Activity levels during the pre-kill phase varied markedly among individuals, ranging from activities with low energetic cost [sit-and-wait (male puma 5M) and slow-walking (female 2F) behaviors] to those with moderate cost [coursing-type movements (16M) and stalk-and-ambush activities (7F)] (Fig. 3). Total energy expended during the pre-kill period (Hunting Cost_{PRE-KILL} in kJ)

decreased with increased use of cryptic behaviors according to

$$\text{Hunting Cost}_{\text{PRE-KILL}} = 3516.0 - 24.9$$

$$(\% \text{time cryptic})$$

$$(r^2 = 0.99, n = 6 \text{ kills}, P < 0.0001) \quad (3)$$

(Fig. 4A). Here, percent time cryptic represents the proportion of the pre-kill period comprising all low-acceleration, low-cost activities [including rest, slow-walking (e.g., stalking), and sit-and-wait behaviors]. Overall, pre-kill hunting costs represented 10 to 20% of the estimated FMR of pumas (13).

Pumas generally remained aerobic during the hunt, only briefly exceeding their predicted $\dot{V}O_{2\text{max}}$ [49.2 to $54.7 \text{ ml O}_2 \text{ kg}^{-1} \text{ min}^{-1}$ (20)] when pouncing. This high-energy activity, along with killing and prey handling, resulted in different acceleration signatures for pumas preying on fawns or bucks (Fig. 3). Predator costs (kJ) are related to prey mass (kg) as

$$\text{Energetic cost of pounce and kill} =$$

$$88.94 - 5.53(\text{prey mass})$$

$$(r^2 = 0.81, n = 5 \text{ known kills}, P = 0.036) \quad (4)$$

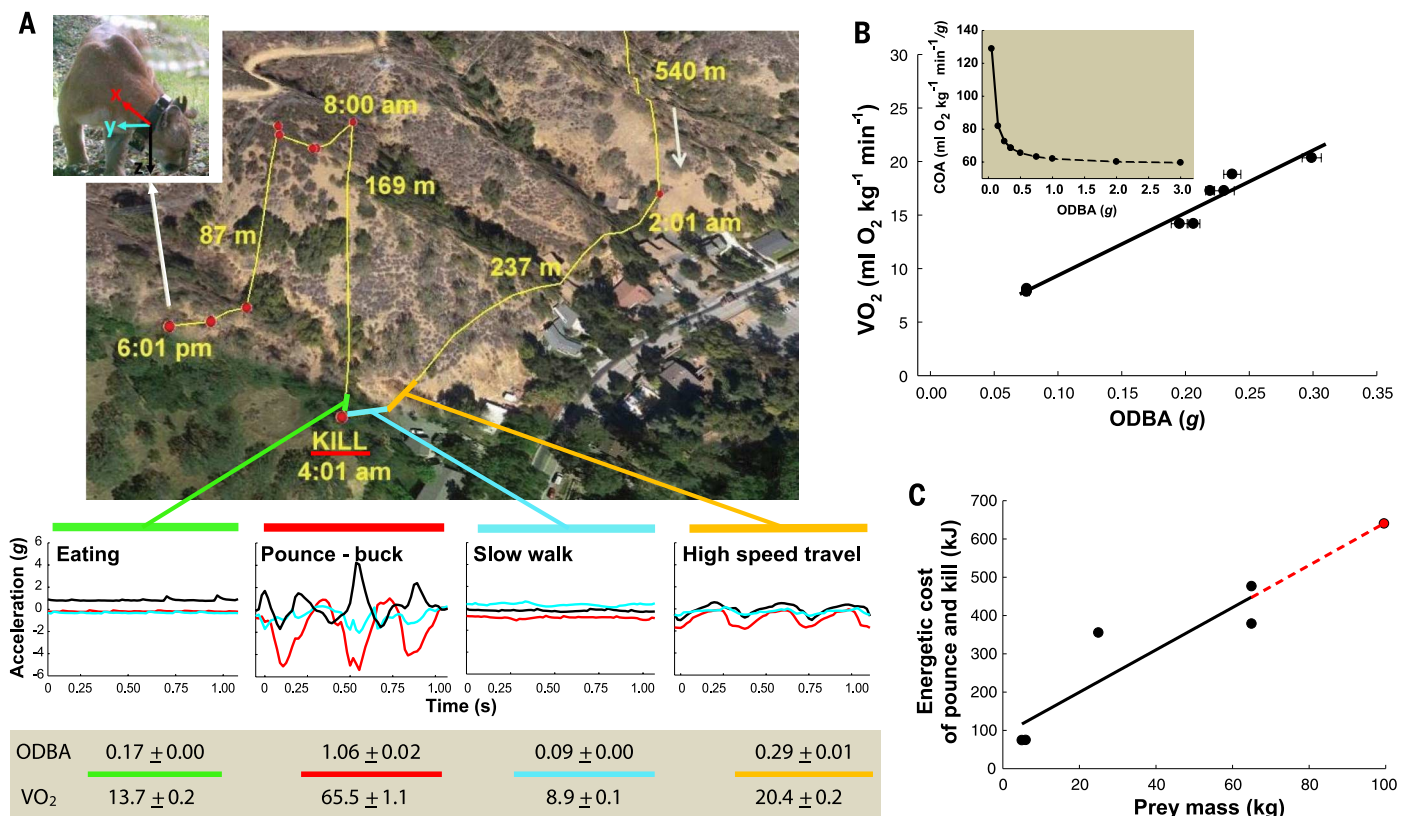


Fig. 2. Field movements, acceleration, and energetic costs for pumas. (A) GPS track for female 13F preying on deer (Google Earth, earth.google.com). Minimum distances moved, time of day, and kill time are indicated. Locations of behavior-specific acceleration signatures ($n = 3840$) (X-surge, red; Y-sway, cyan; Z-heave, black; from collar orientation, inset) are superimposed on the GPS track with corresponding color-coded ODBA (g) and $\dot{V}O_2$ ($\text{ml O}_2 \text{ kg}^{-1} \text{ min}^{-1}$). (B) Relationship between $\dot{V}O_2$ and ODBA for instrumented pumas on a treadmill. Points are mean steady-state measurements ± 1 SE for two pumas. See text for regression (black line) and COA (inset) statistics. (C) Energetic cost of a pounce and kill by pumas in relation to deer mass. Points represent separate kills defined by pounce peak and immediate prey handling (Fig. 3 and table S3). The linear regression (black line, Eq. 4) for five known kills (black symbols) is extrapolated (red dashed line) to predict the size of an unidentified kill according to pounce energetics (red symbol).

mill. Points are mean steady-state measurements ± 1 SE for two pumas. See text for regression (black line) and COA (inset) statistics. (C) Energetic cost of a pounce and kill by pumas in relation to deer mass. Points represent separate kills defined by pounce peak and immediate prey handling (Fig. 3 and table S3). The linear regression (black line, Eq. 4) for five known kills (black symbols) is extrapolated (red dashed line) to predict the size of an unidentified kill according to pounce energetics (red symbol).

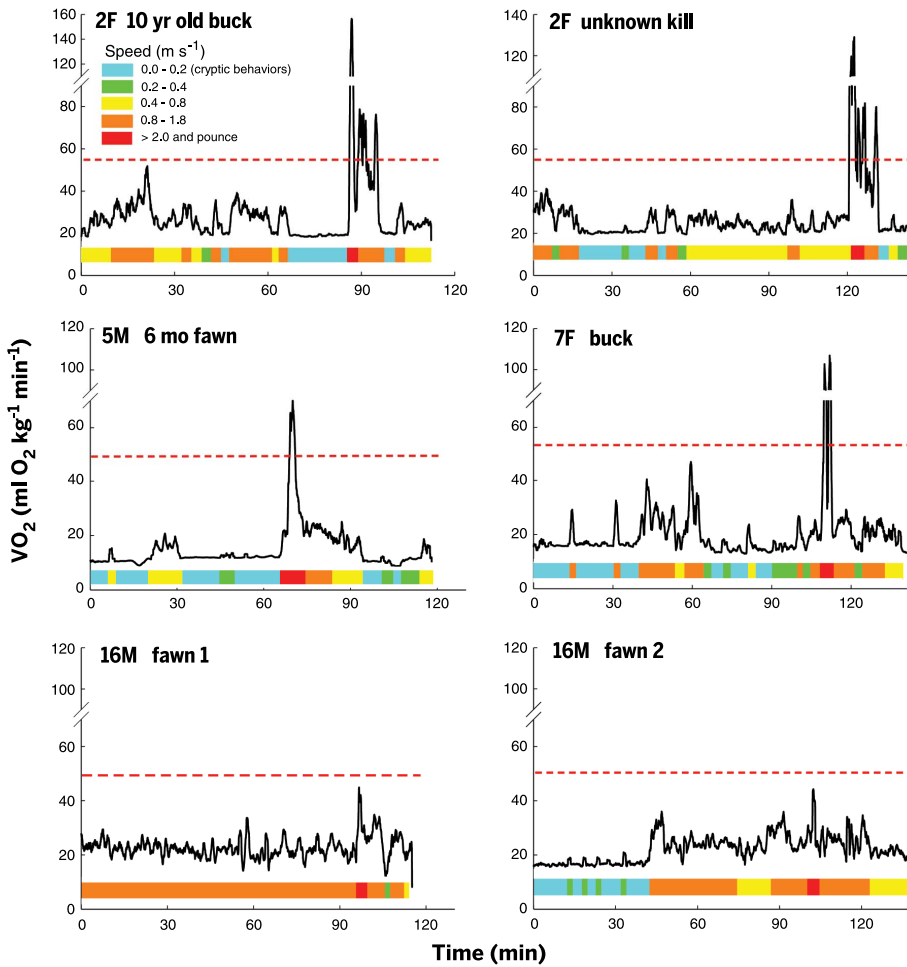


Fig. 3. Activity levels and energetic costs determined from ODBA of wild pumas. Each panel represents a separate kill identified by puma ID and by size and age of the deer. Two-hour hunt segments, including pre-kill, pounce spike, and post-kill prey handling periods, are compared for pumas 2F, 5M, 7F, and 16M. The red dashed line indicates predicted $\dot{V}O_{2\max}$ (20). Colored bars denote speed and behavior according to the inset scale. Low-cost periods (blue bars) were used to calculate percentage of time spent in cryptic activities for each puma.

(Fig. 2C). Extrapolating from this relationship, we estimated the size of an animal that had been attacked, despite being unable to view the event or carcass. Although some prey may be harder to kill and may require more handling than others, pumas appear to precisely gauge the magnitude of the initial pounce to account for the size of the animal to be overtaken (table S3).

We find that the investment of energy for traveling by large terrestrial carnivores is considerable and often underestimated. Comparing pre-kill transport costs for hunting pumas (COT_{HUNT} in $J\ kg^{-1}\ m^{-1}$) to those calculated for foxes (11, 12), wild dogs (10), and tigers (21) results in the allometric regression

$$COT_{\text{HUNT}} = 37.41(\text{mass}^{-0.30})$$

$$(r^2 = 0.74, n = 9 \text{ across 5 species}, P = 0.003)$$

(5)

(Fig. 4B) (13). Energetic demands for pre-kill movements by these large mammalian carnivores average 2.3 times the levels routinely used to model energetic costs from distances moved or GPS tracks (21–23) and 3.8 times the predicted COT_{MIN} (16, 24). These elevated costs undoubtedly reflect the metabolic demands of carnivory (16, 25) as well as the SMART collar’s ability to account for previously overlooked energetic expenditures associated with intermittent locomotion, turning maneuvers, and kinematic changes due to uneven or variable substrates (26–28) that are often imperceptible in most GPS tracks (13). Pumas can mitigate high hunting costs by matching maximum pouncing force to prey size and using cryptic tactics. With such an energetic advantage, it is not surprising that felid morphology and physiology have been shaped over evolutionary time for the stalk-and-pounce sneak attack (5, 6).

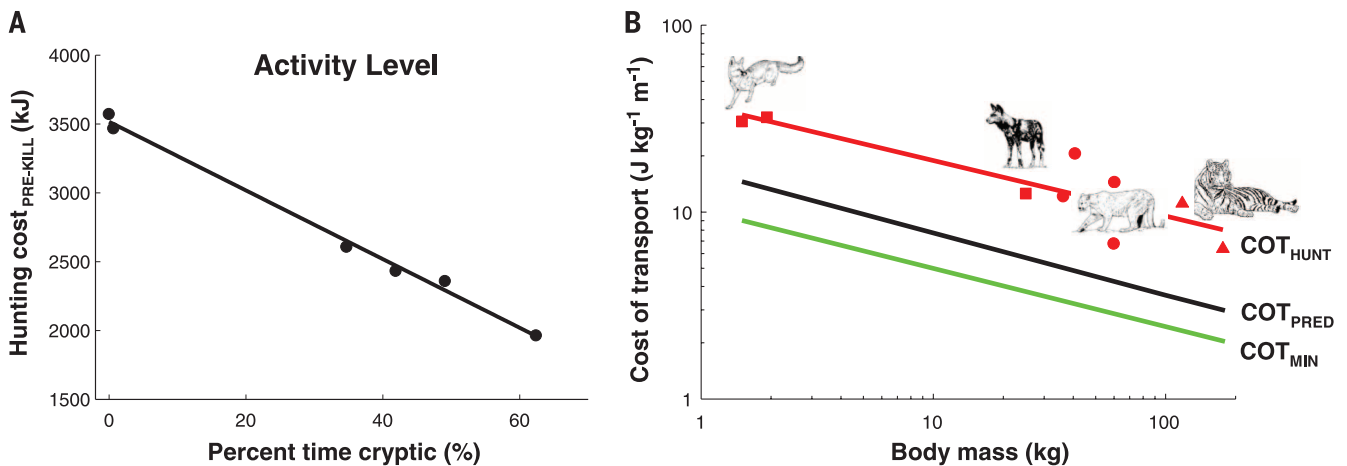


Fig. 4. Effects of behavior and body mass on energetic costs of hunting carnivores. (A) Total energy expended during the pre-kill periods in Fig. 3 in relation to percentage of time pumas spent performing low-activity level (cryptic) behaviors. See text for regression statistics. (B) Minimum (green line from Fig. 1), predicted [black line (14)], and measured (red line, Eq. 5) transport costs for hunting canids (squares) and felids (male and female pumas in this study, circles; male and female tigers, triangles). See supplementary materials for data sources.

Although our study highlights one energetically expensive activity (hunting) for a single carnivore, there are more than 245 mammalian carnivore species (www.iucnredlist.org) and numerous omnivores that pursue and kill mobile, elusive prey. Most have specialized hunting styles and would be expected to display highly variable instantaneous rates of energy expenditure that differ widely among predator and prey, habitats, and even individuals. The laboratory-to-field approach used here, which pairs basic physiological attributes of the animal with standard wildlife monitoring, provides a powerful way of quantifying such species-specific energetic demands. Some activities, including hunting and locomotion across complex habitats, are energetically costly; most are woefully underestimated by many predictive algorithms in common use. Correcting this will become increasingly important for the preservation of large carnivores as foraging becomes progressively affected by continued habitat degradation and loss of vegetative cover essential for cryptic movements (4, 29).

REFERENCES AND NOTES

- D. W. Stephens, J. R. Krebs, *Foraging Theory* (Princeton Univ. Press, Princeton, NJ, 1986).
- R. P. Wilson *et al.*, *J. Anim. Ecol.* **75**, 1081–1090 (2006).
- W. J. Gonyea, *Acta Anat.* **96**, 81–96 (1976).
- M. Sunquist, F. Sunquist, in *Carnivore Behavior, Ecology and Evolution*, J. Gittleman, Ed. (Cornell Univ. Press, Ithaca, NY, 1989), pp. 283–301.
- B. VanValkenburgh, *Paleobiology* **11**, 406–428 (1985).
- D. W. Macdonald, A. J. Loveridge, K. Nowell, in *Biology and Conservation of Wild Felids*, D. Macdonald, A. Loveridge, Eds. (Oxford Univ. Press, Oxford, 2010), pp. 3–58.
- A. M. Wilson *et al.*, *Nature* **498**, 185–189 (2013).
- J. W. Wilson *et al.*, *Biol. Lett.* **9**, 20130620 (2013).
- G. B. Schaller, *The Serengeti Lion* (Univ. of Chicago Press, Chicago, 1972).
- M. L. Gorman, M. G. Mills, J. P. Raath, J. R. Speakman, *Nature* **391**, 479–481 (1998).
- I. Girard, *Physiol. Biochem. Zool.* **74**, 191–202 (2001).
- J. B. Williams, D. Lenain, S. Ostrowski, B. I. Tieleman, P. J. Seddon, *Physiol. Biochem. Zool.* **75**, 479–488 (2002).
- See supplementary materials on Science Online.
- T. M. Williams *et al.*, *Comp. Biochem. Physiol. A* **133**, 203–212 (2002).
- L. Qasem *et al.*, *PLOS ONE* **7**, e31187 (2012).
- C. R. Taylor, N. C. Heglund, G. M. O. Malojo, *J. Exp. Biol.* **97**, 1–21 (1982).
- N. C. Heglund, C. R. Taylor, T. A. McMahon, *Science* **186**, 1112–1113 (1974).
- P. S. Chassin, C. R. Taylor, N. C. Heglund, H. Seeherman, *Physiol. Zool.* **49**, 1–10 (1976).
- L. G. Halsey *et al.*, *Comp. Biochem. Physiol. A* **152**, 197–202 (2009).
- C. R. Taylor *et al.*, *Respir. Physiol.* **44**, 25–37 (1981).
- C. S. Miller *et al.*, *Biol. Conserv.* **170**, 120–129 (2014).
- J. Laundré, L. Hernandez, *J. Arid Environ.* **55**, 675–689 (2003).
- J. Laundré, *J. Wildl. Manage.* **69**, 723–732 (2005).
- C. R. Taylor, K. Schmidt-Nielsen, J. L. Raab, *Am. J. Physiol.* **219**, 1104–1107 (1970).
- B. K. McNab, *Can. J. Zool.* **78**, 2227–2239 (2000).
- O. R. Bidder, L. A. Qasem, R. P. Wilson, *PLOS ONE* **7**, e50556 (2012).
- D. L. Kramer, R. McLaughlin, *Am. Zool.* **41**, 137–153 (2001).
- R. P. Wilson *et al.*, *Ecol. Lett.* **16**, 1145–1150 (2013).
- C. C. Wilmers *et al.*, *PLOS ONE* **8**, e60590 (2013).
- K. Cortis, F. Lindzey, *J. Wildl. Manage.* **48**, 1456–1458 (1984).

ACKNOWLEDGMENTS

Supported by NSF grants DBI-0963022 and 1255913 (T.M.W., C.C.W., and G.H.E.) with in-kind support from the California

Department of Fish and Wildlife. We thank P. Houghtaling, Y. Shakeri, C. Wylie, and D. Tichenor for assistance in catching wild pumas and finding kill sites, and J. A. Estes and the anonymous referees for critical review of this manuscript. Animal procedures were approved by the UCSC IACUC. Statistical data are tabulated in the supplementary materials, with electronic versions available upon request from the senior author through the UCSC Mammal Physiology Project database.

SUPPLEMENTARY MATERIALS

www.sciencemag.org/content/346/6205/81/suppl/DC1
Materials and Methods
Tables S1 to S3
References (31–38)

16 April 2014; accepted 30 July 2014
10.1126/science.1254885

PROSTATE CANCER

Ubiquitylome analysis identifies dysregulation of effector substrates in SPOP-mutant prostate cancer

Jean-Philippe P. Theurillat,^{1,2,3*} Namrata D. Udeshi,^{1*} Wesley J. Errington,^{4,5*} Tanya Svinkina,¹ Sylvan C. Baca,^{2,3} Marius Pop,^{1,2,3} Peter J. Wild,⁶ Mirjam Blattner,⁷ Anna C. Groner,³ Mark A. Rubin,^{7,8} Holger Moch,⁶ Gilbert G. Privé,^{4,5} Steven A. Carr,¹ Levi A. Garraway^{1,2,3,9,†}

Cancer genome characterization has revealed driver mutations in genes that govern ubiquitylation; however, the mechanisms by which these alterations promote tumorigenesis remain incompletely characterized. Here, we analyzed changes in the ubiquitin landscape induced by prostate cancer–associated mutations of SPOP, an E3 ubiquitin ligase substrate-binding protein. SPOP mutants impaired ubiquitylation of a subset of proteins in a dominant-negative fashion. Of these, DEK and TRIM24 emerged as effector substrates consistently up-regulated by SPOP mutants. We highlight DEK as a SPOP substrate that exhibited decreases in ubiquitylation and proteasomal degradation resulting from heteromeric complexes of wild-type and mutant SPOP protein. DEK stabilization promoted prostate epithelial cell invasion, which implicated DEK as an oncogenic effector. More generally, these results provide a framework to decipher tumorigenic mechanisms linked to dysregulated ubiquitylation.

Genome sequencing studies have revealed unanticipated roles for the ubiquitylation machinery in cancer. For example, the cullin-RING ubiquitin ligase adaptor protein speckle-type POZ protein (SPOP) is mutated in 8 to 14% of prostate and endometrial cancers (1–4). In prostate cancer, SPOP mutations are confined to specific amino acid residues within the substrate-binding cleft, which mediates substrate interaction and ubiquitin transfer (5). This exquisite localization suggests that SPOP mutations have undergone positive selection during tumorigenesis by altering binding and ubiquitylation of distinct effector substrates in a protumorigenic manner. However, the mecha-

nisms and substrates underlying this phenomenon remain incompletely understood.

In principle, mutant SPOP could enhance ubiquitylation of SPOP substrates (gain-of-function effect) or ubiquitylate new substrates (neomorphic effect). Alternatively, SPOP mutants could dimerize with their wild-type counterparts (e.g., through the BTB and BACK domains), and so repress wild-type SPOP function (dominant-negative effect). In support of the latter model, SPOP mutations typically occur in a heterozygous state with a retained wild-type allele and are able to dysregulate known substrates [e.g., nuclear receptor coactivator 3 (NCOA3)] in a dominant-negative manner (1, 6).

Characterizing the ubiquitin landscape (or “ubiquitylome”) that results from cancer genomic alterations affecting ubiquitin ligase components may provide new insights into tumorigenesis. To interrogate changes in ubiquitylation conferred by prostate cancer SPOP mutations, we stably overexpressed vector control (C); wild-type SPOP (SPOP-WT); or a mutated variant (SPOP-F133L or SPOP-Y87N, in which Phe¹³³ is replaced by Leu or Tyr⁸⁷ is replaced by Asn (SPOP-MT)), in immortalized prostate epithelial cells expressing endogenous SPOP (fig. S1, A and B) (7). In each case, we characterized the resulting ubiquitylome by measuring glycine-glycine remnants of ubiquitylated lysines (K-ε-GG) after

¹The Broad Institute of Harvard and MIT, Cambridge, MA 02142, USA. ²Harvard Medical School, Boston, MA 02115, USA.

³Department of Medical Oncology, Dana-Farber Cancer Institute, Boston, MA 02115, USA. ⁴Department of Biochemistry, University of Toronto, Toronto, Ontario M5S 1A8, Canada.

⁵Princess Margaret Cancer Centre, University Health Network, Toronto, Ontario M5G 2M9, Canada. ⁶Institute of Surgical Pathology, University Hospital Zurich, ZH 8091 Zurich, Switzerland. ⁷Department of Pathology and Laboratory Medicine, Weill Cornell Medical College, New York, NY 10065, USA. ⁸Institute for Precision Medicine of Weill Cornell and New York Presbyterian Hospital, New York, NY 10065, USA. ⁹Center for Cancer Genome Discovery, Dana-Farber Cancer Institute, Boston, MA 02115, USA.

*These authors contributed equally to this work. †Corresponding author. E-mail: levi_garraway@dfci.harvard.edu